Interactions of pulmonary surfactant protein SP-A with monolayers of dipalmitoylphosphatidylcholine and cholesterol: roles of SP-A domains

Shou-Hwa Yu,[1,*,§] Francis X. McCormack,[**] Dennis R. Voelker,[††] and Fred Possmayer[*,†,§]

Department of Obstetrics and Gynecology,* Department of Biochemistry,[†] and MRC Group in Fetal and Neonatal Health and Development,[§] University of Western Ontario, 339 Windermere Road, London, Ontario, Canada N6A 5A5; Division of Pulmonary and Critical Care Medicine,** Department of Medicine, University of Cincinnati, Cincinnati, OH 45267-0564; and Department of Medicine,[††] Anna Perahia Adatto Clinical Research Center, National Jewish Center for Immunology and Respiratory Medicine, Denver, CO 80206

Abstract **Pulmonary surfactant protein A (SP-A) is an oligomeric glycoprotein that binds dipalmitoylphosphatidylcholine (DPPC). Interactions of rat SP-A and recombinant SP-As with pure and binary monolayers of DPPC and cholesterol were studied using a rhomboid surface balance at 37°C. A marked inflection at equilibrium surface tension (23 mN/m) in surface tension-area isotherm of a pure DPPC film was abolished by rat SP-A. The inflection was decreased and shifted to 18 mN/m with wild-type recombinant SP-A (SP-A^{hyp}). Both rat SP-A and SP-A^{hyp} decreased surface area reduction required for pure DPPC films to reach near zero surface tension from 30 to 25%. SP-A^{hyp,E195Q,R197D}, mutated in carbohydrate recognition domain (CRD) known to be essential for SP-A–vesicle interactions, conveyed a detrimental effect on DPPC surface activity. SP-A$^{\Delta G8\text{-}P80}$, with deletion of collagen-like domain, had little effect. Both SP-A^{hyp,C6S} (Ser substitution for Cys^{6}) and SP-A$^{hyp,\Delta N1\text{-}A7}$ (N-terminal segment deletion) which appear mainly as monomers on non-reducing SDS-PAGE analysis, increased required surface area reduction for minimal surface tension. All SP-As reduced collapse surface tension of a pure cholesterol film from 27 to 23 mN/m in the presence of Ca^{2+}. When mixed films were formed by successive spreading of DPPC/SP-A/cholesterol, rat SP-A, SP-A^{hyp}, or SP-A$^{\Delta G8\text{-}P80}$ blocked the interaction of cholesterol with DPPC; SP-A^{hyp,E195Q,R197D} could not impede the interaction; SP-A^{hyp,C6S} or SP-A$^{hyp,\Delta N1\text{-}A7}$ only partially blocked the interaction, and cholesterol appeared to stabilize SP-A^{hyp,C6S}–DPPC association. These results demonstrate the importance of CRD and N-terminal dependent oligomerization in SP-A–phospholipid associations. The findings further indicate that SP-A–cholesterol interactions differ from SP-A–DPPC interactions and may be nonspecific.**—Yu, S-H., F. X. McCormack, D. R. Voelker, and F. Possmayer. **Interactions of pulmonary surfactant protein SP-A with monolayers of dipalmitoylphosphatidylcholine and cholesterol: roles of SP-A domains.** ***J. Lipid Res.*** **1999.** 40: **920–929.**

Supplementary key words air/water interface • monolayer • DPPC • SP-A • cholesterol • L-B film

Pulmonary surfactant is composed of about 90% lipids and 10% proteins with dipalmitoylphosphatidylcholine (DPPC) as the major lipid component. The main function of pulmonary surfactant is to maintain the stability of the lung by reducing the surface tension at the air/alveoli interface (1–3). Surfactant protein A (SP-A) is an abundant surfactant protein in the alveoli (4, 5). SP-A is a hydrophilic glycoprotein with a monomeric molecular mass of 28,000–36,000 dalton (6, 7). SP-A belongs to the C-type (Ca^{2+}-dependent) carbohydrate binding protein family (8, 9) and shares extensive sequence homology with mannose binding protein A (10). An SP-A monomer consists of four structural domains (11). Analysis of rat SP-A revealed (12): *1*) a disulfide bond-forming amino terminal segment (Asn^{1}–Ala^{7}); *2*) a collagen-like domain (Gly^{8}–Pro^{80}); *3*) a hydrophobic neck region (Gly^{78}–Val^{114}); *4*) a carbohydrate recognition domain (CRD), (Gly^{115}–Phe^{228}). In its native state, SP-A assembles into oligomers as a consequence of non-covalent trimerization of the collagen and neck domains. Further oligomeric assembly occurs by covalent crosslinking of trimers to form an octadecamer with a bouquet-like structure similar to that of C1q (13, 14). In the presence of Ca^{2+}, SP-A induces the aggregation of phospholipid vesicles (15, 16) and has a high affinity toward DPPC (17, 18). Recombinant wild-type rat SP-A and several mutant SP-As have been produced in insect cells using recombinant baculoviruses and characterization of their biological functions indicates that the CRD is essential for SP-A to interact with phospholipid vesicles (12, 19).

Abbreviations: DPPC, dipalmitoylphosphatidylcholine; L-B film, Langmuir-Blodgett film; PL, phospholipid; BLES, bovine lipid extract surfactant; SP- surfactant associated protein; PAGE, polyacrylamide gel electrophoresis; CRD, carbohydrate recognition domain.

[1] To whom correspondence should be addressed.

Pulmonary surfactant contains 4–7% neutral lipid, mainly cholesterol. Although cholesterol decreases the gel-to-liquid crystalline transition temperature of DPPC in aqueous dispersions and increases the re-entry of DPPC into monolayers (20), it impairs the surface tension-lowering ability of the surfactant. Several studies (21–23) have shown that in the absence of SP-A, cholesterol cannot be readily squeezed out from the mixed films through repeated compression.

Previously we reported that bovine SP-A can decrease the collapse surface tension of pure cholesterol monolayers and facilitate the squeeze-out of cholesterol from DPPC/cholesterol mixed monolayers, which were formed with the successive spreading of DPPC/SP-A /cholesterol, by limiting the interaction of cholesterol with DPPC (24). It is clear from those studies (24) that SP-A can interact directly with cholesterol in pure cholesterol monolayers and with DPPC in pure or mixed monolayers. However, it is not clear whether SP-A also interacted directly with cholesterol in mixed monolayers or which SP-A domain was associated with cholesterol. In the present study we used several mutant SP-As to evaluate the roles of individual structural domains of SP-A in interactions with DPPC and cholesterol.

MATERIALS AND METHODS

Materials

Dipalmitoyl-1-[^{14}C]phosphatidylcholine was purchased from New England Nuclear (Markham, Ontario, Canada). DPPC and cholesterol were from Sigma Chemical Co.(Mississauga, Ontario, Canada). The Bicinchoninic Acid Protein Assay (BCA) Kit was from Pierce. All reagents and other chemicals (analytical grade) were from BDH (British Drug House Inc., Toronto). Distilled water purified through a Millipore Milli-Q four-cartridge system was used in all experiments.

Purification of rat SP-A

Rat SP-A was isolated from bronchoalveolar lavage of Sprague-Dawley rats 4 weeks after the intratracheal instillation of 40 mg/kg of silica. The protein was purified by delipidation with butanol, affinity chromatography using mannose–Sepharose 6B and size fractionation by Bio-Gel A-15 m gel permeation chromatography as described previously (25).

Production of recombinant SP-A^{hyp}, SP-A^{hyp,E195Q,R197D}, SP-A$^{\Delta G8\text{-}P80}$, SP-A^{hyp,C6S}, and SP-A$^{hyp,\Delta N1\text{-}A7}$

The mutant recombinant proteins used in this study have been previously reported and will be only briefly outlined here. Mutant cDNAs encoding the substitutions Glu 195 to Gln (26), and Arg197 to Asp (26), Cys6 to Ser (27), the deletion of amino acids Gly8–Pro80 (27), and the deletion of Asn1–Ala7 (28) were produced from the 1.6 kb rat SP-A cDNA template by overlapping extension PCR (29). The mutated cDNAs were ligated into the Eco R1 site of PVL 1392 transfer vector and the correct orientations were confirmed by endonuclease digestion with Kpn 1 and electrophoretic analysis. Nucleotide sequencing of the entire coding region (30) for all constructs confirmed the intended substitutions and deletions, and the absence of spurious mutations. Recombinant baculoviruses containing the mutant cDNAs were produced by homologous recombination in *Spodoptera frugiperda* (Sf-9) cells after contransfection with linear viral DNA (Baculogold, Pharmingen) and the PVL 1392/mutant SP-A constructs, as described. Fresh monolayers of 107 *Trichoplusia Ni* (T. Ni) cells were infected with plaque-purified recombinant viruses at a multiplicity of infection of 10, and then incubated with serum-free media (IPL-41) supplemented with 0.4 mm ascorbic acid and antibiotics for 72 h. Recombinant SP-A was purified from the culture media by adsorption to mannose–Sepharose 6B columns in the presence of 1 mm Ca^{2+} and elution with 2 mm EDTA (31). The purified recombinant SP-A was dialyzed against 5 mm Tris (pH 7.4) and stored at −20°C.

Protein assays

Purified rat SP-A and recombinant SP-As, originally stored in aqueous media at −20°C, were thawed and dissolved in water–2-propanol 2:1 before experiments. These proteins were subsequently stored in water–2-propanol 2:1 at −20°C where the protein solutions do not freeze, and analyzed in a 12.5% SDS-polyacrylamide gel electrophoresis (PAGE) gel (32). Protein concentrations were estimated with a BCA Protein Assay Kit using bovine serum albumin as a standard.

Preparation of bovine lipid extract surfactant containing cholesterol, BLES(chol)

BLES(chol) was extracted from bovine natural surfactant by the procedure of Bligh and Dyer as previously described (33). BLES(chol) retains all protein and lipid components of natural surfactant except SP-A.

Pulsating bubble surfactometer

Effects of SP-A^{hyp} on the surface activity of BLES(chol) at 30° and 37°C were examined using a pulsating bubble surfactometer (34). Briefly, a bubble of 0.55 mm diameter with interface of air/BLES(chol) dispersion (1 mg/ml) was pulsated between 0.55–0.40 mm at 20 rpm. The pressure (Δp) across the bubble was measured with a transducer and the surface tension was calculated by Laplace equation $\Delta p = 2\partial/r$ where ∂ is the surface tension and r is the radius of the bubble.

Surface tension–surface area measurements

A rhomboid surface balance (24) was used to study the surface tension–area isotherms of pure and binary mixed monolayers of DPPC and cholesterol in the presence and absence of SP-A at 37°C. In a typical experiment, 120 ml saline containing 1.5 mm $CaCl_2$ was poured into a trough which was placed on a temperature-regulated hot plate (37 ± 0.5°C) and enclosed in a temperature-controlled box (37 ± 0.5°C). A 5-mm wide platinum plate was dipped into the subphase and the surface tension was monitored with a TSAR 1 computer-controlled readout (TECH-SER, Inc., Torrance, CA). A sample of DPPC or cholesterol in hexane–methanol 95:5 was spread on the subphase to a desired surface tension. A dynamic compression from a surface area of 24 to 10 cm^2 was initiated after 15 min of solvent evaporation at 60 mm/min. In the experiments including SP-A, a 30 μl solution of 0.4 mg/ml SP-A in water–2-propanol 2:1 was applied onto several locations of the lipid monolayer after a 15-min pause for solvent evaporation. With all mixed monolayers studied, the components were spread successively in the sequence of DPPC/cholesterol or DPPC/SP-A/cholesterol. In each case, a dynamic compression was begun 30 min after the sample application was completed. The initial surface tension of DPPC was 30–31 mN/m and the concentration of cholesterol was 3.5 wt% of DPPC.

Surface active properties of SP-A at 37°C were also examined using the rhomboid surface balance. A small amount of SP-A, ranging from 2 to 4 μg in 0.4 mg/ml water–2-propanol 2:1, was applied on a surface area of 24 cm^2 subphase and the initial surface tension was 70 mN/m. The compression procedure was car-

ried out as described above. Calculation of the area per amino acid was based on the assumption of a molecular mass of 35,000 dalton and 228 residues per monomer of SP-A (7, 12).

Langmuir-Blodgett (L-B) films deposition and autoradiography

L-B films of DPPC in the presence of rat SP-A or recombinant SP-As were deposited on a 1 × 1 cm^2 microscope glass cover slip at equilibrium surface tension (~23 mN/m) using the rhomboid surface balance at 37°C as described previously (24). Briefly, 30 μl of 0.4 mg/ml SP-A in water–2-propanol 2:1 was applied onto several locations of a ^{14}C-labeled DPPC monolayer with a surface tension of 30–31 mN/m. Thirty minutes after sample application, the monolayer was compressed slowly at 0.8 mm/min. An L-B film was deposited on the glass plate, which was lowered into the subphase of saline, 1.5 mm $CaCl_2$ prior to the spreading of DPPC, by lifting the plate up slowly at 1 mm/min when the surface tension reached 23 mN/m. The surface tension was maintained constant throughout the deposition process. The specific radioactivity of all samples was 3 μCi/mg DPPC. Autoradiographs of L-B films were produced by exposing the plates to X-ray films for about 40 h at 4°C.

RESULTS AND DISCUSSION

SDS-PAGE analysis of SP-As

Recombinant SP-As, expressed in insect cells using baculovirus vectors, contain less hydroxyproline in the collagen-like domains than rat SP-A recovered from lavage and these proteins are designated SP-A^{hyp} (25). Hydroxyproline stabilizes the triple-helical structure of collagen by forming hydrogen bonds between hydroxyl groups (35). As a result, wild-type recombinant SP-A^{hyp} is not as stable as rat SP-A at physiological temperatures. In this study four additional variants of SP-A were used: *1*) SP-$A^{hyp,E195Q,R197D}$ was produced by substitution of Glu^{195} with Gln and Arg^{197} with Asp to alter the carbohydrate binding specificity of SP-A^{hyp} from mannose to galactose (36); *2*) SP-$A^{\Delta G8\text{-}P80}$ has a deletion of the collagen-like domain (27); *3*) SP-$A^{hyp,C6S}$, serine substitutes for Cys^6 to prevent the formation of interchain-disulfide bonds (27); *4*) SP-$A^{hyp,\Delta N1\text{-}A7}$ has a deletion of the amino terminal segment (28). Coomassie blue staining of SP-A variants after electrophoresis under non-reducing conditions is shown in **Fig. 1**. These SP-As were stored unfrozen in water–2-propanol 2:1 at −20°C. Figure 1 reveals that electrophoretic profiles of SP-As stored in propanol solutions were similar to those of SP-As stored in an aqueous solvent under non-reducing conditions (26, 27). Rat SP-A (lane a) appeared as multiple bands of dimers and oligomers. SP-A^{hyp} (lane b) formed monomers, dimers, and oligomers. SP-$A^{hyp,E195Q,R197D}$ (lane c) formed protein bands similar to those of SP-A^{hyp}. SP-$A^{\Delta G8\text{-}P80}$ (lane d) appeared to be mostly dimers and tetramers. SP-$A^{hyp,C6S}$ (lane e) showed mainly monomers and SP-$A^{hyp,\Delta N1\text{-}A7}$ (lane f) revealed monomers and a small amount of dimers. Both SP-$A^{hyp,C6S}$ and SP-$A^{hyp,\Delta N1\text{-}A7}$ lack interchain-disulfide bonds adjacent to the collagen-like domains essential for covalent oligomerization and stabilizing the triple helical structures (37). An additional disulfide forming cysteine

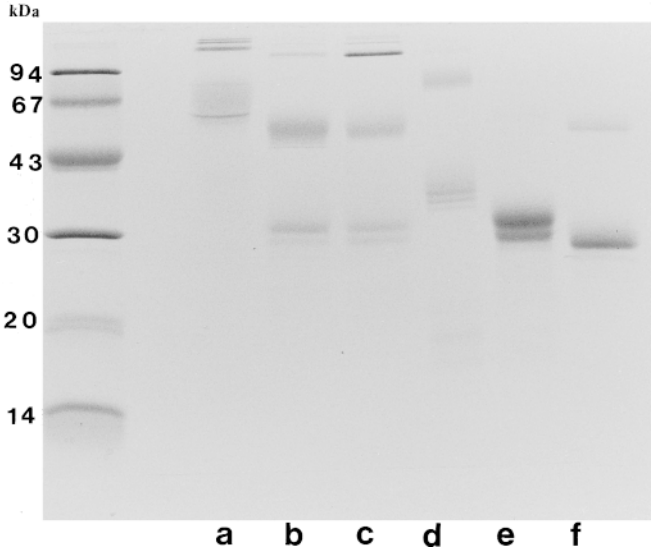

Fig. 1. SDS-PAGE analysis of SP-As. Electrophoresis was conducted using a 4% stacking and a 12.5% separating gel under non-reducing conditions. Protein-bands were stained with Coomassie brilliant blue: a, rat SP-A; b, SP-A^{hyp}; c, SP-$A^{hyp,E195Q,R197D}$; d, SP-$A^{\Delta G8\text{-}P80}$; e, SP- $A^{hyp,C6S}$; f, SP-$A^{hyp,\Delta N1\text{-}A7}$.

recently identified as Cys^{-1} is also present in a minor isoform of rat SP-A and recombinant SP-A that has an extra three amino acids at the N-terminus (28).

It is known that self-aggregation of SP-A occurs in aqueous medium with various concentrations of Ca^{2+} depending on the species (38, 39). These non-covalent aggregates will not be seen in non-reducing SDS-PAGE as the aggregates are dispersed by SDS. In the present studies all SP-As were dissolved in water–2-propanol 2:1; it is highly unlikely that SP-As aggregate in this solution.

Surface-active properties of rat SP-A and SP-A^{hyp}

Surface-active properties of native SP-A and recombinant SP-A were assessed with the rhomboid surface balance at 37°C. **Figure 2** shows that rat SP-A did not reduce the surface tension of the air/saline, 1.5 mm $CaCl_2$ interface when the surface area was compressed from 24 to 10 cm^2. This result suggests that rat SP-A did not form an insoluble monolayer at the interface and was not surface active. Identical experiments with bovine SP-A revealed the same result (results not shown). These findings are consistent with our earlier observations indicating that bovine SP-A is not surface active (24). However, surface tension at the interface was moderately reduced when SP-A^{hyp} was applied onto the surface and compressed. This may be due to differences in protein-folding between native rat SP-A and SP-A^{hyp}, and is possibly related to the deficiency of hydroxyproline in SP-A^{hyp}. SDS-PAGE analysis shows that the degree of oligomerization in SP-A^{hyp} is not as complete as in rat SP-A (Fig. 1 lanes a and b). These observations differ from previous studies which reported the formation of an insoluble film at the air/saline interface for native porcine SP-A dissolved in 5 mm HEPES, 0.1% amyl alcohol or 1-propanol–0.5 m sodium acetate 1:1 at 22 ± 2°C (40).

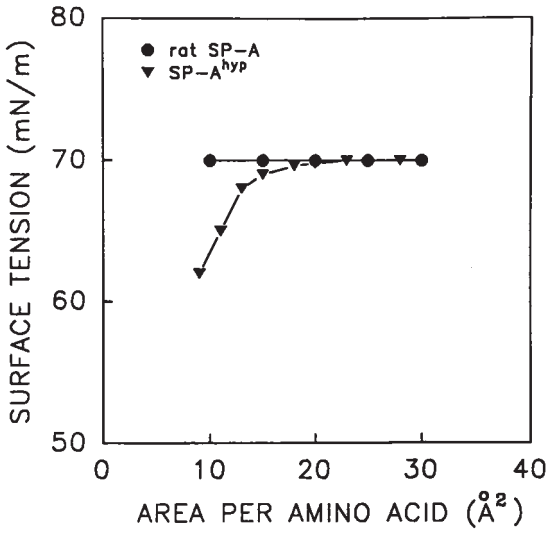

Fig. 2. Surface-active properties of rat SP-A and SP-A^{hyp}. Isotherms of surface tension–surface area at 37°C were obtained using a rhomboid surface balance as described in the text.

Effect of temperature on the ability of SP-A^{hyp} to enhance the surface activity of BLES(chol)

To assess the thermal stability of SP-A^{hyp}, the effects of SP-A^{hyp} on the surface activities of BLES(chol) at 30° and 37°C were measured with a bubble pulsating surfactometer. **Figure 3** shows that the surface activities of BLES(chol) at 1 mg/ml were similar at 30° and 37°C. Addition of SP-A^{hyp} enhanced the surface activity of BLES(chol). The surface activity was increased more at 30°C than at 37°C with 2% SP-A^{hyp}. This could be attributed to the thermal instability of the collagen-like domain due to deficiency of hydroxyproline (25). However, with 5% SP-A^{hyp}, minimum surface tension was attained within 60 pulsations at 37°C. These results demonstrate that a moderate concentration of SP-A^{hyp} can effectively enhance the surface activity of BLES(chol) at 37°C.

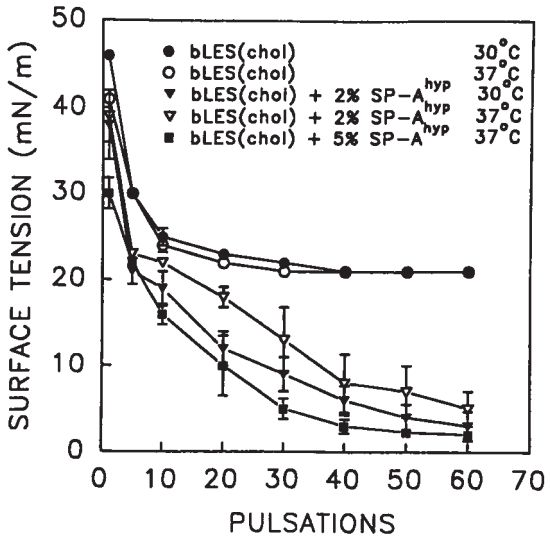

Fig. 3. Effect of temperature on SP-A^{hyp} in enhancing surface activity of BLES(chol). Surface tension lowering properties of BLES(chol) in the absence and presence of SP-A^{hyp} at 30 and 37°C were conducted using a pulsating bubble surfactometer. Concentration of BLES(chol) was 1 mg/ml in saline, 1.5 mm $CaCl_2$. Data are mean ± SE for n = 3.

Interaction of rat SP-A or SP-A^{hyp} with DPPC at the air/saline, 1.5 mM $CaCl_2$ interface

The effect of rat SP-A or SP-A^{hyp} on the surface area reduction required for a pure DPPC film to reach near zero surface tension was investigated by applying SP-A on a preformed DPPC monolayer at 30 mN/m. **Figure 4** illustrates the surface tension–surface area isotherms of DPPC films in the presence and absence of SP-A at 37°C. A marked inflection was observed around equilibrium surface tension (23 mN/m) in the compression curve for a pure DPPC monolayer. We previously interpreted the appearance of the inflection as an indication of the loss of monolayer material during compression (24). However, it is also possible that the inflection results from conformational changes in the head groups of DPPC. It has been reported that DPPC head groups can be rearranged by compressing the monolayer (41) and the tilted hydrocarbon-chain conformation is determined by the orientation of the head groups (42). Watkins (43) has observed a decrease in the slope of a surface potential–surface area isotherm for a pure DPPC monolayer at the point corresponding to the onset of the inflection in the surface tension–surface area isotherm. He suggested that the inflection was a result of changes in the orientation of the choline and phosphate groups of DPPC from co-planar with the surface to coaxial with the hydrocarbon chains during compression of the DPPC monolayer. As a result, the hydrocarbon chains of DPPC became more condensed. Figure 4 and **Table 1**, row 1, also show that pure DPPC films attained near zero surface tension with 30% surface area reduction from equilibrium surface tension and sustained the over-

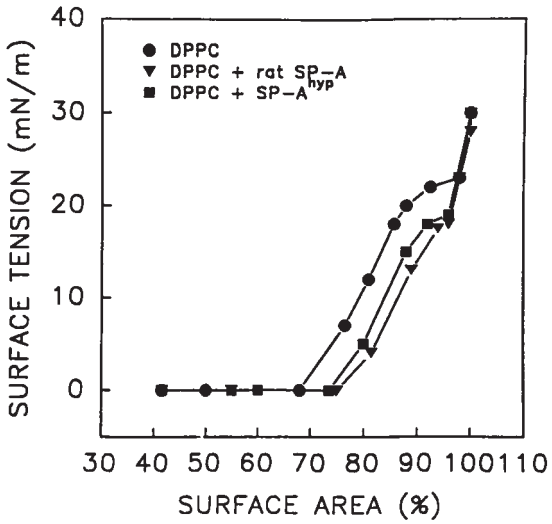

Fig. 4. Representative surface tension–surface area isotherms for pure DPPC films in the presence and absence of rat SP-A or SP-A^{hyp} at 37°C. Experiments were carried out as described in the text.

TABLE 1. Interactions of SP-A with pure DPPC and mixture of DPPC/Cholesterol at the air/water interface

Monolayers[a]	Initial Surface Tension[b]	Reduction of Surface Area Required from 23 mN/m to Near Zero Surface Tension[c]	Significance[d]
	mN/m	*%*	*P*
1. DPPC	30–31	30.2 ± 0.9	
2. DPPC + CHOL	30–31 → 26–27	>60	
3. DPPC + rat SP-A	30–31 → 28–29	24.8 ± 0.8	$P_{1,3} < 0.05$
4. DPPC + rat SP-A + CHOL	30–31 → 28–29 → 24–25	25.3 ± 0.7	$P_{3,4} > 0.05$
5. DPPC + SP-A^{hyp}	30–31 → 30–31	25.0 ± 1.2	$P_{1,5} < 0.05$
6. DPPC + SP-A^{hyp} + CHOL	30–31 → 30–31 → 26–27	25.5 ± 0.8	$P_{5,6} > 0.05$
7. DPPC + SP-A^{hyp,E195Q,R197D}	30–31 → 30–31	>50	
8. DPPC + SP-A^{hyp,E195Q,R197D} + CHOL	30–31 → 30–31 → 26–27	>60	
9. DPPC + SP-A$^{\Delta G8\text{-}P80}$	30–31 → 30–31	28.9 ± 0.5	$P_{1,9} > 0.05$
10. DPPC + SP-A$^{\Delta G8\text{-}P80}$ + CHOL	30–31 → 30–31 → 26–27	28.0 ± 1.0	$P_{9,10} > 0.05$
11. DPPC + SP-A^{hyp,C6S}	30–31 → 30–31	40.7 ± 1.2	$P_{1,11} < 0.05$
12. DPPC + SP-A^{hyp,C6S} + CHOL	30–31 → 30–31 → 26–27	32.0 ± 2.0	$P_{11,12} < 0.05$
13. DPPC + SP-A$^{hyp,\Delta N1\text{-}A7}$	30–31 → 30–31	35.6 ± 2.6	$P_{1,13} < 0.05$
14. DPPC + SP-A$^{hyp,\Delta N1\text{-}A7}$ + CHOL	30–31 → 30–31 → 26–27	46.8 ± 1.2	$P_{13,14} < 0.05$

Dynamic compressions at the air/saline, 1.5 mm $CaCl_2$ interface were performed from the surface area of 24 to 10 cm^2 at 6 cm/min and 37°C.

[a] Composition of a monolayer is expressed in the order of the successive spreading of each component.

[b] Initial surface tension of DPPC in all samples was 30–31 mN/m. Arrows indicate the surface tensions at the air/saline, 1.5 mm $CaCl_2$ interfaces after the successive spreading of SP-A or cholesterol. All monolayers of DPPC plus cholesterol contain 3.5 wt % cholesterol.

[c] Data are mean ± SE for n ⩾ 3.

[d] *P* values were obtained from a two-tailed *t*-test. Differences were significant when $P < 0.05$.

compression past collapse. With over-compression, DPPC films buckle and form overlapping layers at the interface (44); the surface tension remains constant at near zero during this process.

Observations from our earlier monolayer studies (24) suggested that bovine SP-A preferentially interacted with the head groups of DPPC monolayers. Figure 4 reveals that addition of rat SP-A to a DPPC monolayer at 30 mN/m nearly abolished the inflection and the surface area reduction required to reach near zero surface tension was decreased from 30 to 25%, similar to that observed previously with bovine SP-A (24). The disappearance of the inflection at 23 mN/m is likely due to the changes in conformation of the DPPC head groups adopted at 30 mN/m when SP-A was applied onto the DPPC monolayer. As a result, the area reduction required to attain near zero surface tension was reduced.

Interaction of SP-A^{hyp} with DPPC shifted the diminished inflection to 18 mN/m. This result suggests that SP-A^{hyp} also altered the conformation of DPPC head groups before compression but to a lesser extent than rat SP-A, and further conformational changes occurred upon compression to 18 mN/m. Nonetheless, the surface area reduction required to reach near zero surface tension for DPPC films in the presence of SP-A^{hyp} was similar to rat SP-A. Both SP-As reduced the required surface area reduction for DPPC films from 30% (in the absence of SP-A) to 25% (in the presence of SP-A). Similar to bovine SP-A (24), addition of rat SP-A to a DPPC monolayer at 30 mN/m reduced the surface tension slightly to 28 mN/m. But the surface tension remained constant upon addition of SP-A^{hyp} as shown in Table 1, rows 3 and 5. These results also demonstrate the possible alteration in conformation of DPPC monolayers upon the addition of rat SP-A at 30 mN/m. As a result, the surface tension was reduced moderately. Whereas SP-A^{hyp} may also alter the orientation of DPPC molecules, the effect was less than with rat SP-A and was not strong enough to alter the surface tension.

The interactions of SP-As with DPPC monolayers at the equilibrium surface tension (23 mN/m) are also analyzed with L-B films. **Figure 5** shows that at 37°C both rat SP-A (A) and SP-A^{hyp} (B) are capable of inducing the aggregation of DPPC molecules at 23 mN/m, but to different extents.

Addition of SP-A^{hyp} to vesicles composed of DPPC–egg PC–egg phosphatidylglycerol (PG) 9:3:2 resulted in vesicle aggregations at 20°C but not at 37°C (27). The vesicle–vesicle interactions observed under these conditions are dependent on SP-A–SP-A associations, and are likely different from the DPPC aggregation observed with monolayers.

Interactions of SPAs with cholesterol

Cholesterol forms a liquid condensed monolayer with the molecules perpendicularly oriented at the interface at all surface tensions; therefore cholesterol has very little compressibility (45, 46). It has a relatively high equilibrium surface tension of 33–34 mN/m and collapses at 27–28 mN/m upon compression at 37°C or 30°C. **Table 2** compiles the effects of SP-A and individual structural domains of SP-A on the collapse surface tension of pure cholesterol monolayers in the presence and absence of Ca^{2+} at 37°C. The results showed that rat SP-A, SP-A^{hyp}, and all mutant SP-As tested clearly reduced the collapse surface tension to 23 mN/m in the presence of Ca^{2+}. These findings imply that the interactions of SP-A with cholesterol do not require any of the specific domains evaluated in this report, although the association is Ca^{2+} dependent.

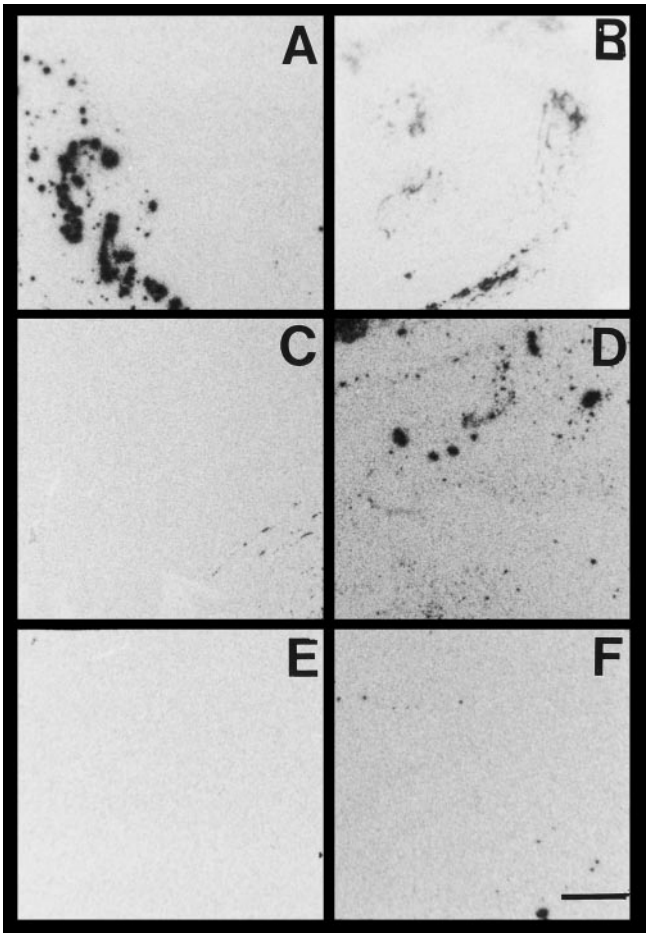

Fig. 5. Autoradiographs of L-B films deposited with [^{14}C]DPPC-labeled pure DPPC films at 23 mN/m and 37°C in the presence of SP-A. A, rat SP-A; B, SP-A^{hyp}; C, SP-A^{hyp,E195Q,R197D}; D, SP-A$^{\Delta G8\text{-}P80}$; E, SP-A^{hyp,C6S}; F, SP-A$^{hyp,\Delta N1\text{-}A7}$. The bar indicates 2 mm in all graphs. The films presented are typical of films from three experiments.

These data indicate that the SP-A–cholesterol interactions are different from the SP-A–DPPC interactions. As cholesterol orients vertically at the interface with the β-OH moiety below the interface, it seems reasonable to suggest that hydrogen-bonding between the sterol and protein is responsible for the decrease in collapse surface tension. However, rat SP-A did not aggregate cholesterol at its equilibrium surface tension (33–34 mN/m) nor did it affect the aggregation of cholesterol molecules formed below the equilibrium surface tension; aggregates of cholesterol in L-B films formed around 30 mN/m appeared to be similar in the presence and absence of SP-A (results not shown).

Interaction of rat SP-A or SP-A^{hyp} with mixed monolayers of DPPC and cholesterol

Cholesterol condenses PC monolayers (21) and preferentially interacts with disaturated PC (47). It has been proposed that hydrogen bond formation between the β-hydroxyl hydrogen of cholesterol and the carbonyl oxygen of DPPC is essential for the interaction (48). Previously we have shown (24) that successive spreading of DPPC and 3.5 wt% cholesterol at the air/saline, 1.5 mm $CaCl_2$ interface resulted in the formation of cholesterol-rich domains which may mimic the organization of biological membranes (49, 50). Cholesterol is a major component of mammalian plasma membranes. It plays important roles in the growth and function of mammalian cells, such as influencing membrane permeability and stability, and regulating plasma membrane protein activity and membrane biosynthesis (51). Although the function of cholesterol in the pulmonary surfactant system is not clear, it has been observed that cholesterol enhances transport of DPPC to the surface from a surfactant dispersion and increases the reservoir of DPPC below the interface (33). Cholesterol also improves re-spreading of DPPC into the air/water interface (20). However, in a mixed monolayer of DPPC and cholesterol, cholesterol impaired the surface tension lowering ability of DPPC (24). **Figure 6A** and Table 1, row 2, show that DPPC/cholesterol mixed monolayers, formed by successive spreading, required the maximum compression to reach near zero surface tension at 37°C. We have demonstrated that bovine SP-A was able to pre-

TABLE 2. Interactions of SP-A with cholesterol at the air/water interface

Monolayers[a]	Initial Surface Tension[b]	Ca^{2+}	Collapse Surface Tension[c]	*P* Values[d]
	mN/m		*mN/m*	
1. CHOL	37–38	+	27.5 ± 0.3	
	37–38	−	27.0 ± 0.5	
2. CHOL + rat SP-A	37–38 → 35–36	+	22.6 ± 0.5	$P_{1,2} < 0.05$
	37–38 → 35–36	−	27.6 ± 0.4	
3. CHOL + SP-A^{hyp}	37–38 → 37–38	+	22.7 ± 0.6	$P_{1,3} < 0.05$
	37–38 → 37–38	−	27.4 ± 0.6	
4. CHOL + SP-A^{hyp,E195Q,R197D}	37–38 → 37–38	+	23.0 ± 0.2	$P_{1,4} < 0.05$
5. CHOL + SP-A$^{\Delta G8–P80}$	37–38 → 37–38	+	22.8 ± 0.4	$P_{1,5} < 0.05$
6. CHOL + SP-A^{hyp,C6S}	37–38 → 37–38	+	22.5 ± 0.5	$P_{1,6} < 0.05$
7. CHOL + SP-A$^{hyp,\Delta N1–A7}$	37–38 → 37–38	+	22.8 ± 0.4	$P_{1,7} < 0.05$

Experiments were carried out as in Table 1 except that some experiments were performed in the absence of $CaCl_2$.

[a] Composition of monolayers corresponds to the spreading order of each component.

[b] Arrows indicate the surface tensions after the successive application of SP-A.

[c] Data are mean ± SE for n ⩾ 3.

[d] Differences were analyzed using a two-tailed *t*-test.

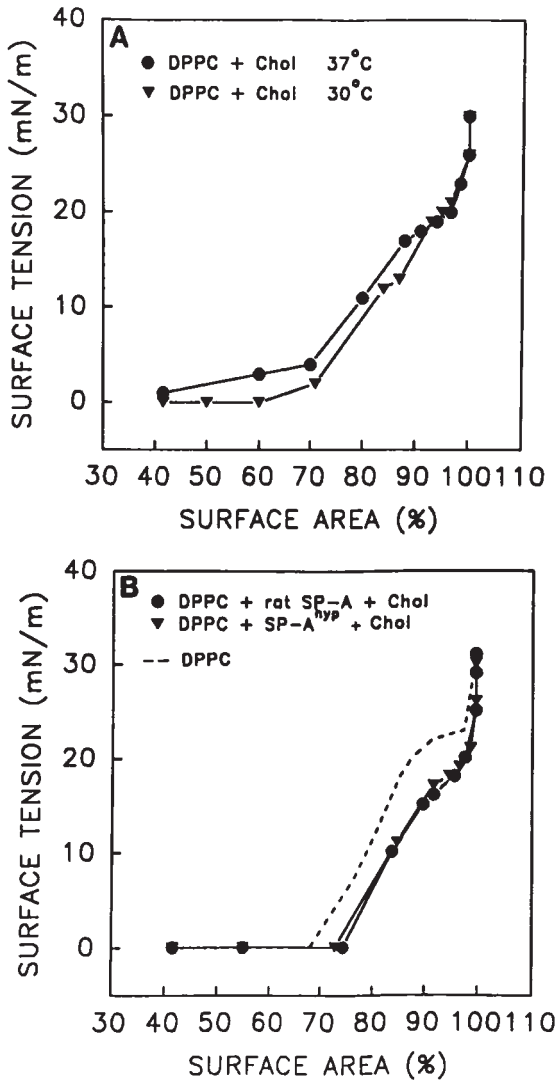

Fig. 6. A: Surface tension–surface area isotherms for mixed films of DPPC and cholesterol at 30° and 37°C. DPPC and cholesterol were dissolved separately in hexane–methanol 95:5. Cholesterol (3.5 wt%) was spread on a preformed DPPC monolayer at 30 mN/m. B: Representative dynamic compression curves for mixed films of DPPC and cholesterol in the presence of rat SP-A or SP-A^{hyp} at 37°C. Mixed films were formed by the successive spreading of DPPC, SP-A, and cholesterol.

vent the detrimental effect of cholesterol on the surface-active property of DPPC, apparently by interacting with DPPC first and blocking the interaction of cholesterol with DPPC (24). Figure 6A also reveals that a DPPC/cholesterol mixed monolayer, formed by successive spreading, could reach near zero surface tension with about 40% area reduction at 30°C. However, when mixed monolayers were formed by co-spreading of DPPC and cholesterol, similar results were observed at 30° and 37°C. The mixed films required the maximum compression (~65%) to reach very low surface tension (results not shown).

In the present study we also performed successive spreading of DPPC/SP-A/cholesterol to examine the effect of SP-A on the surface properties of mixed films. Figure 6B shows similar surface tension–area isotherms were obtained with DPPC/rat SP-A/cholesterol and DPPC/SP-A^{hyp}/cholesterol mixed films at 37°C. Both rat SP-A and SP-A^{hyp} were able to impede the interaction of cholesterol with DPPC and restore the surface area reduction required to achieve near zero surface tension by compressing only 25% with these mixed films (Table 1, rows 4 and 6). This suggests that under these experimental conditions SP-A^{hyp} is functionally comparable to rat SP-A, and can therefore serve as a basis for comparison with mutant proteins used to assess the role of individual structural domains in SP-A–DPPC monolayer interactions. Figure 6B also reveals that the small inflection in the compression curve of DPPC/SP-A^{hyp} was further reduced by addition of cholesterol (compare Fig. 4 with Fig. 6B). This could be the result of condensing effect of cholesterol on DPPC molecules which had not interacted with SP-A^{hyp}. Our previous results (24) indicated that SP-A preferentially interacts with DPPC head groups in DPPC monolayers and addition of cholesterol to DPPC films in the presence of SP-A does not affect SP-A–DPPC interactions. We conclude that cholesterol does not associate with rat SP-A or SP-A^{hyp} that had interacted with DPPC in the mixed films for the following reasons: *1*) the effects of SP-A on the surface activities of DPPC were similar in the presence and absence of cholesterol; *2*) the aggregation of DPPC induced by SP-A was similar in the presence and absence of cholesterol (24); *3*) it is likely that the vertical orientation of SP-A introduced by the multivalent binding of the CRD to the head groups of DPPC in mixed films places SP-A oligomers in positions that are not structurally compatible with binding to the β-OHs of cholesterol immediately below the surface.

Interactions of SP-A^{hyp,E195Q,R197D} with monolayers of pure DPPC and mixtures of DPPC and cholesterol

SDS-PAGE analysis reveals that SP-A^{hyp} and SP-A^{hyp,E195Q,R197D} have identical migration profiles (Fig. 1). This result showed that substitution of Glu^{195} with Gln and Arg^{197} with Asp in the CRD did not affect the overall covalent oligomerization of SP-A. However, these alterations greatly affected the interaction of SP-A with DPPC as this mutant does not induce the aggregation of DPPC (Fig. 5C). **Figure 7** shows that addition of SP-A^{hyp,E195Q,R197D} onto DPPC monolayers impaired the surface tension-lowering ability of DPPC. The inflection in the compression curve for SP-A^{hyp,E195Q,R197D} was more apparent than with SP-A^{hyp}. Furthermore, the DPPC film required near maximum compression to reach low surface tension and the resulting film was very unstable. These results showed that SP-A^{hyp,E195Q,R197D} interacted with DPPC in a manner that did not enhance the surface tension-lowering effects of the film during compression, possibly by preventing the normal orientation of DPPC molecules at the interface as DPPC films seemed unable to sustain low surface tension during compression in the presence of SP-A^{hyp,E195Q,R197D}. Upon over-compression, it is likely that DPPC molecules were squeezed out from the film into the subphase, resulting in rising surface tension.

Figure 7 also shows that the compression curve for

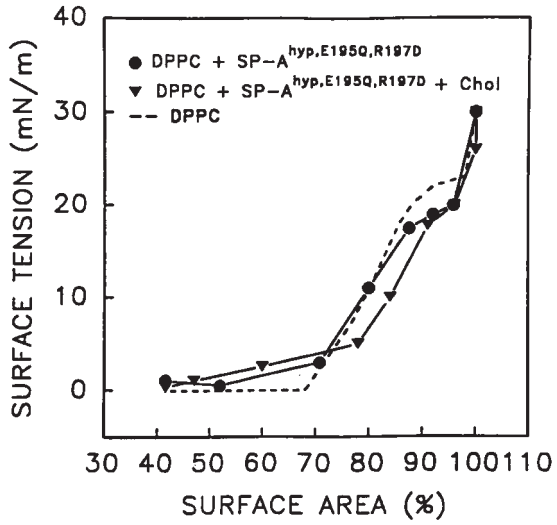

Fig. 7. Representative dynamic compression curves for pure DPPC and mixed DPPC/cholesterol films in the presence of SP-A^{hyp,E195Q,R197D} at 37°C.

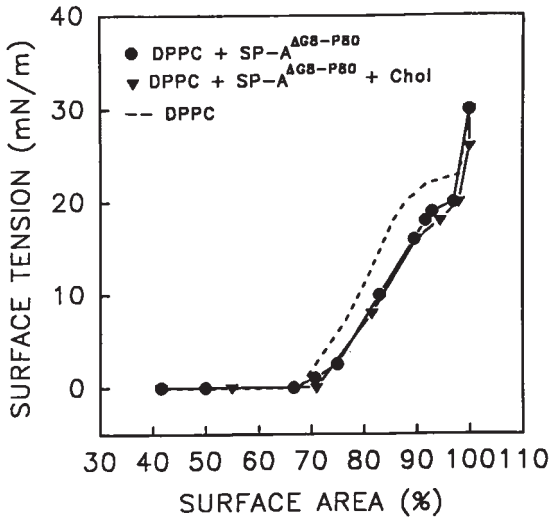

Fig. 8. Representative dynamic compressive curves of pure DPPC and mixture of DPPC and cholesterol in the presence of SP-A$^{\Delta G8\text{-}P80}$ at 37°C.

DPPC/SP-A^{hyp,E195Q,R197D}/cholesterol had a trend similar to that for DPPC/cholesterol at 37°C (Fig. 6 A). Collectively the data indicate that SP-A^{hyp,E195Q,R197D} could neither block the interaction of cholesterol with DPPC nor interact directly with cholesterol. We conclude that the CRD of SP-A is required for SP-A to bind with DPPC in a proper orientation thereby enhancing the surface activity of DPPC monolayers.

Interactions of SP-A$^{\Delta G8\text{-}P80}$ with monolayers of pure DPPC and mixtures of DPPC and cholesterol

SP-A$^{\Delta G8\text{-}P80}$, lacks the collagen-like domain but forms disulfide-linked dimers and oligomers (Fig.1 lane d). At 37°C, SP-A$^{\Delta G8\text{-}P80}$ also aggregated DPPC molecules in the monolayer although not as extensively as rat SP-A (Fig. 5D). We have previously reported that, like SP-A^{hyp}, SP-A$^{\Delta G8\text{-}P80}$ aggregates vesicles composed of DPPC–egg PC–egg PG 9:3:2 at 20°C but not at 37°C (27). **Figure 8** and Table 1, row 9, show that SP-A$^{\Delta G8\text{-}P80}$ slightly improved the surface activity of pure DPPC monolayers, but the effect was not significant. The results also showed that SP-A$^{\Delta G8\text{-}P80}$ could prevent the negative effect of cholesterol on the surface activity of DPPC in mixed films (Fig. 8 and Table 1, row 10). This indicates that SP-A$^{\Delta G8\text{-}P80}$ could directly interact with DPPC and effectively block the interaction of cholesterol with DPPC. In the presence of SP-A$^{\Delta G8\text{-}P80}$, surface activities of DPPC appeared to be similar with and without cholesterol (Table 1, rows 9 and 10), indicating that SP-A$^{\Delta G8\text{-}P80}$ did not interact with cholesterol in the mixed films.

Interactions of SP-A^{hyp,C6S} with monolayers of pure DPPC and mixtures of DPPC and cholesterol

On SDS-PAGE analysis, the SP-A^{hyp,C6S} is mainly composed of monomers and lesser amounts of dimeric species (Fig. 1, lane e). SP-A^{hyp,C6S} did not aggregate DPPC molecules at equilibrium surface tension and 37°C (Fig. 5E). **Figure 9** shows that SP-A^{hyp,C6S} greatly reduced the surface tension-lowering ability of DPPC films. The surface area reduction required for reducing the surface tension to near zero was increased from 30 to 40% by the addition of SP-A^{hyp,C6S} to a DPPC monolayer. However, films were stable at near zero surface tension and could withstand overcompression. This may relate to the fact that SP-A^{hyp,C6S} possesses a wild-type CRD binding site but exhibits low affinity toward DPPC, perhaps due to incomplete oligomeric assembly. Addition of cholesterol to DPPC films in the presence of SP-A^{hyp,C6S} significantly enhanced the surface activity of the mixed films, insofar as the surface area reduction required for minimal surface tension was decreased from 40 to 32% (Table 1, rows 11 and 12). These results suggest that SP-A^{hyp,C6S} could interact with DPPC

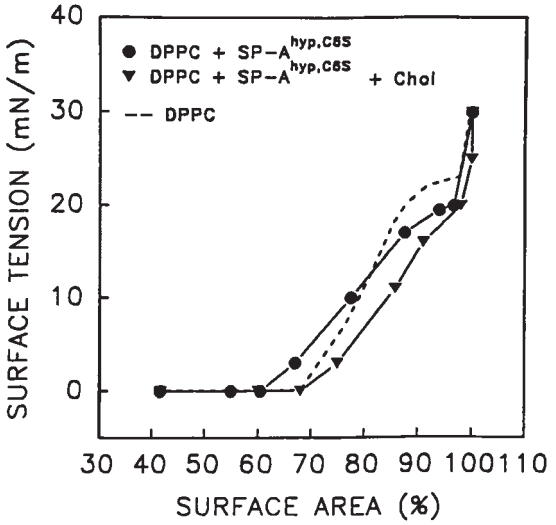

Fig. 9. Representative dynamic compression curves for pure DPPC and DPPC/cholesterol mixed films in the presence of SP-A^{hyp,C6S} at 37°C.

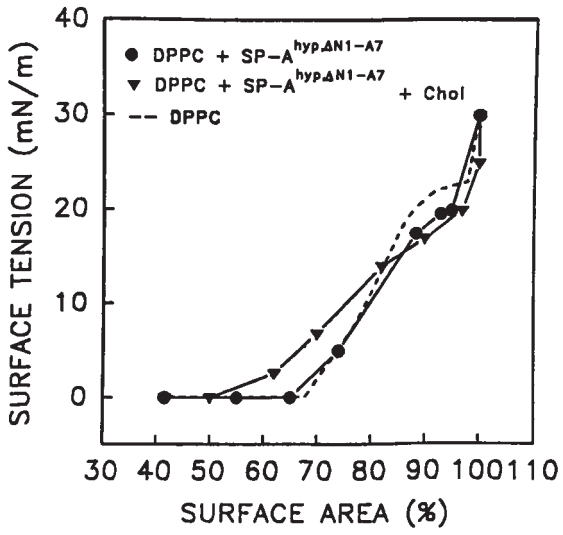

Fig. 10. Representative dynamic compression curves for pure DPPC and DPPC/cholesterol mixture in the presence of SP-A$^{hyp,\Delta N1\text{-}A7}$ at 37°C.

and block the interaction of cholesterol with DPPC in the mixed films. Furthermore, cholesterol appears to stabilize SP-A^{hyp,C6S}–DPPC interactions. Although the mechanism is not known, this could be the result of interactions between cholesterol and SP-A^{hyp,C6S}.

Interactions of SP-A$^{hyp,\Delta N1\text{-}A7}$ with monolayers of pure DPPC and mixtures of DPPC/cholesterol

Figure 10 and Table 1, row 13, show that DPPC molecules exhibited more stable interactions with SP-A$^{hyp,\Delta N1\text{-}A7}$ than with SP-A^{hyp,C6S}. Although both mutant SP-As lacked Cys^{6} interchain–disulfide bonds, SP-A$^{hyp,\Delta N1\text{-}A7}$ formed more dimers than SP-A^{hyp,C6S} did by virtue of greater interchain–disulfide formation at Cys^{-1} (Fig. 1, lanes e and f). However, SP-A$^{hyp,\Delta N1\text{-}A7}$ was also unable to aggregate DPPC at the equilibrium surface tension at 37°C (Fig. 5F) and failed to aggregate phospholipid vesicles (results not shown).

When cholesterol was added onto the DPPC film in the presence of SP-A$^{hyp,\Delta N1\text{-}A7}$, this protein could not prevent the detrimental effect of cholesterol on the surface activity of DPPC (Fig. 10 and Table 1, row 14). These results indicate that SP-A$^{hyp,\Delta N1\text{-}A7}$ could interact with DPPC but was relatively weak at preventing the interaction of cholesterol with DPPC. There was no evidence for an interaction between SP-A$^{hyp,\Delta N1\text{-}A7}$ and cholesterol. The observations that cholesterol could stabilize the mixed films in the presence of SP-A^{hyp,C6S} which possesses the amino terminal segment but not in the presence of SP-A$^{hyp,\Delta N1\text{-}A7}$ which lacks the amino terminal segment, indicate that the amino terminal domain is important for the interaction between SP-A^{hyp,C6S} and cholesterol in a mixed film.

In summary, we have shown that at 37°C the wild-type recombinant SP-A, SP-A^{hyp}, is functionally comparable to rat SP-A in enhancing the surface activity of pure DPPC films as well as in preventing the detrimental effects of cholesterol on the surface activity of DPPC films by inhibiting the interaction of cholesterol with DPPC. Mutant SP-A with altered carbohydrate recognition specificity binds DPPC but severely impairs the surface tension-lowering ability of DPPC films. In contrast, the collagen domain deletion mutant does not perturb the surface activity of DPPC but prevents cholesterol from inhibiting the surface activity. Mutant SP-As that alter N-terminal SP-A structure and reduce covalent oligomerization also diminish the surface activity of DPPC films but provide weak protection from cholesterol inactivation. These results suggest that the CRD is required for SP-A–DPPC monolayer associations, while the remaining domains are involved in oligomeric assembly that impart a higher affinity and appear to strengthen SP-A–DPPC interactions by supporting multivalent binding. All SP-As studied reduce the collapse surface tension of pure cholesterol films from 27 to 23 mN/m. On the contrary, none of the SP-As except SP-A^{hyp,C6S} appear to associate with cholesterol in mixed films formed by successive spreading of DPPC/SP-A/cholesterol.

This work was supported by an MRC Group Grant from the Medical Research Council of Canada, and grants from the American Lung Association, the Department of Veterans Affairs, and the National Institutes of Health.

Manuscript received 3 September 1998 and in revised form 7 January 1999.

REFERENCES

1. Keough, K. M. W. 1992. Physical chemistry of pulmonary surfactant in terminal air spaces. *In* Pulmonary Surfactant. B. Robertson, L. M. G. Van Golde and J. J. Batenberg, editors. Elsevier, The Netherlands. 109–164.
2. Goerke, J. 1992. Surfactant and lung mechanics. *In* Pulmonary Surfactant. B. Robertson, L. M. G. Van Golde and J. J. Batenburg, editors. Elsevier, The Netherlands. 165–187.
3. Possmayer, F. 1997. Physicochemical aspects of pulmonary surfactant. *In* Fetal and Neonatal Physiology. R. A. Polin and W. H. Fox, editors. W. B. Sanders, Philadelphia. Chapter 115: 1259–1275.
4. Sueishi, K., and B. J. Benson. 1981. Isolation of a major apolipoprotein of canine and murine pulmonary surfactant. *Biochim. Biophys. Acta.* **665:** 442–453.
5. Yu, S. H., N. Smith, P. G. R. Harding, and F. Possmayer. 1983. Bovine pulmonary surfactant: chemical composition and physical properties. *Lipids.* **18:** 522–529.
6. Whitsett, J. A., W. Hull, G. Ross, and T. Weaver. 1985. Characteristics of human surfactant-associated glycoproteins A. *Pediatr. Res.* **19:** 501–508.
7. Hawgood, S., and K. Shiffer. 1991. Structures and properties of surfactant-associated proteins. *Annu. Rev. Physiol.* **53:** 375–394.
8. Weis, W. I., and K. Drickamer. 1996. Structural basis of lectin-carbohydrate recognition. *Annu. Rev. Biochem.* **65:** 441–473.
9. Haagsman, H. P., S. Hawgood, T. Sargeant, D. Buckley, R. T. White, K. Drickamer, and B. J. Benson. 1987. The major lung surfactant protein, SP 28-36, is a calcium-dependent, carbohydrate-binding protein. *J. Biol. Chem.* **262:** 13877–13880.
10. Drickamer, K., M. S. Dordal, and L. Reynolds. 1986. Mannose-binding proteins isolated from rat liver contain carbohydrate-recognition domains linked to collagenous tails. *J. Biol. Chem.* **261:** 6878–6887.
11. White, R. T., D. Damm, J. Miller, K. Spratt, J. Schilling, S. Hawgood, B. Benson, and B. Cordell. 1985. Isolation and characterization of human pulmonary surfactant apoprotein gene. *Nature.* **317:** 361–363.
12. McCormack, F. 1997. The structure and function of surfactant protein-A. *Chest.* **111:** 114S–119S.
13. Voss, T., H. Eistetter, and K. P. Schäfer. 1988. Macromolecular organization of natural and recombinant lung surfactant protein SP 28-36. *J. Mol. Biol.* **201:** 219–227.

14. King, R. J., D. Simon, and P. M. Horowitz. 1989. Aspects of secondary and quarternary structure of surfactant protein A from canine lung. *Biochim. Biophys. Acta.* **1001:** 294–301.
15. King, R. J., and M. C. MacBeth. 1981. Interaction of the lipid and protein components of pulmonary surfactant: Role of phosphatidylglycerol and calcium. *Biochim. Biophys. Acta.* **647:** 159–168.
16. Hawgood, S., B. J. Benson, and R. L. Hamilton, Jr. 1985. Effects of a surfactant-associated protein and calcium ions on the structure and surface activity of lung surfactant lipids. *Biochemistry.* **24:** 184–190.
17. Kuroki, Y., and T. Akino. 1991. Pulmonary surfactant protein A (SP-A) specifically binds dipalmitoylphosphatidylcholine. *J. Biol. Chem.* **266:** 3068–3073.
18. King, R. J., M. C. Carmichael, and P. M. Horowitz. 1983. Reassembly of lipid-protein complexes of pulmonary surfactant. *J. Biol. Chem.* **258:** 10672–10680.
19. Kuroki, Y., F. X. McCormack, Y. Ogasawara, R. J. Mason, and D. R. Voelker. 1994. Epitope mapping for monoclonal antibodies identifies functional domains of pulmonary surfactant protein A that interact with lipids. *J. Biol. Chem.* **269:** 29793–29800.
20. Notter, R. H., S. A. Tabak, and R. D. Mavis. 1980. Surface properties of binary mixtures of some pulmonary surfactant components. *J. Lipid Res.* **21:** 10–22.
21. Shah, D. O., and J. H. Schulman. 1967. Influence of calcium, cholesterol and unsaturation on lecithin monolayers. *J. Lipid Res.* **8:** 215–225.
22. Yu, S. H., and F. Possmayer. 1994. Effect of pulmonary surfactant protein A (SP-A) and calcium on the adsorption of cholesterol and film stability. *Biochim. Biophys. Acta.* **1211:** 350–358.
23. Wang, Z., S. B. Hall, and R. H. Notter. 1995. Dynamic surface activity of films of lung surfactant phospholipids, hydrophobic proteins, and neutral lipids. *J. Lipid Res.* **36:** 1283–1293.
24. Yu, S. H., and F. Possmayer. 1998. Interaction of pulmonary surfactant protein A with dipalmitoylphosphatidylcholine and cholesterol at the air/water interface. *J. Lipid Res.* **39:** 555–568.
25. McCormack, F. X., H. M. Calvert, P. A. Watson, D. L. Smith, R. J. Mason, and D. R. Voelker. 1994. The structure and function of surfactant protein A: hydroxyproline and carbohydrate-deficient mutant proteins. *J. Biol. Chem.* **269:** 5833–5841.
26. McCormack, F. X., Y. Kuroki, J. J. Stewart, R. J. Mason, and D. R. Voelker. 1994. Surfactant protein A amino acids Glu^{195} and Arg^{197} are essential for receptor binding, phospholipid aggregation, regulation of secretion, and the facilitated uptake of phospholipid by type II cells. *J. Biol. Chem.* **269:** 29801–29807.
27. McCormack, F. X., S. Pattanajitvilai, J. Stewart, F. Possmayer, K. Inchley, and D. R. Voelker. 1997. The Cys^{6} intermolecular disulfide bond and collagen-like region of rat SP-A play critical roles in interactions with alveolar type II cells and surfactant lipids. *J. Biol. Chem.* **272:** 27971–27979.
28. Elhalwagi, B. M., M. Damodarasamy, and F. X. McCormack. 1997. Alternate amino terminal processing of surfactant protein A results in cysteinyl isoforms required for multimer formation. *Biochemistry.* **36:** 7018–7025.
29. Horton, R. M., H. D. Hunt, S. N. Ho, J. K. Pullen, and L. R. Pease. 1989. Engineering hybrid genes without the use of restriction enzymes: gene splicing by overlap extension. *Gene (Amst)* **77:** 61–68.
30. Sanger, F., S. Nicklen, and A. R. Coulson. 1977. DNA sequencing with chain-terminating inhibitors. *Proc. Natl. Acad. Sci. USA.* **74:** 5463–5467.
31. Fornstedt, N., and J. Porath. 1975. Characterization studies on a new lectin found in seeds of *Vicia ervilia. FEBS Lett.* **57:** 189–191.
32. Laemmli, U. K. 1970. Cleavage of structural proteins during the assembly of the head of bacteriophage T_4. *Nature.* **227:** 680–685.
33. Yu, S. H., and F. Possmayer. 1996. Effect of pulmonary surfactant protein A and neutral lipid on accretion and organization of dipalmitoylphosphatidylcholine in surface films. *J. Lipid Res.* **37:** 1278–1288.
34. Enhorning, G. 1977. Pulsating bubble technique for evaluating pulmonary surfactant. *J. Appl. Physiol.* **43:** 198–203.
35. Ramachandran, G. M., and A. H. Reddi. 1976. Biochemistry of Collagen. Plenum Press, New York. 67–71.
36. Drickamer, K. 1992. Engineering galactose-binding activity into a C-type mannose-binding protein. *Nature.* **360:** 183–186.
37. Hass, C., T. Voss, and J. Engel. 1991. Assembly and disulfide rearrangement of recombinant surfactant protein A in vitro. *Eur. J. Biochem.* **197:** 799–803.
38. Haagsman, H. P., T. Sargeant, P. V. Hauschka, B. J. Benson, and S. Hawgood. 1990. Binding of calcium to SP-A, a surfactant-associated protein. *Biochemistry.* **29:** 8894–8900.
39. Miguel, L. F. R., E. Miguel, J. Perez-Gil, and C. Casals. 1996. Comparison of lipid aggregation and self-aggregation activities of pulmonary surfactant-associated protein A. *Biochem. J.* **313:** 683–689.
40. Taneva, S., T. McEachren, J. Stewart, and K. M. W. Keough. 1995. Pulmonary surfactant protein SP-A with phospholipids in spread monolayers at the air-water interface. *Biochemistry.* **34:** 10279–10289.
41. Adam, N. K. 1941. Surface films of insoluble substances. *In* Physics and Chemistry of Surface. Oxford University Press, New York. 46–55.
42. Alexander, A. E. 1942. A proposed general structure for condensed monomolecular films. *Proc. R. Soc. (London)* **A 179:** 486–498.
43. Watkins, J. C. 1968. The surface properties of pure phospholipids in relation to those of lung extracts. *Biochim. Biophys. Acta.* **152:** 293–306.
44. Tchoreloff, P., A. Gulik, B. Denizot, J. E. Proust, and F. Puisenx. 1991. A structural study of interfacial phospholipid and lung surfactant layers by transmission electron microscopy after Blodgett sampling: influence of surface pressure and temperature. *Chem. Phys. Lipids.* **59:** 151–165.
45. Pethica, B. A. 1955. The thermodynamics of monolayer penetration at constant area. *Trans. Faraday Soc.* **51:** 1402–1411.
46. Demel, R. A., and B. De Kruyff. 1976. The function of sterols in membranes. *Biochim. Biophys. Acta.* **457:** 109–132.
47. Guyer, W., and K. Bloch. 1983. Phosphatidylcholine and cholesterol interactions in model membranes. *Chem. Phys. Lipids.* **33:** 313–322.
48. Blockhoff, H. 1974. Model of interaction of polar lipids, cholesterol, and proteins in biological membranes. *Lipids.* **9:** 645–650.
49. Liscum, L., and K. W. Underwood. 1995. Intracellular cholesterol transport and compartmentation. *J. Biol. Chem.* **270:** 15443–15446.
50. Glaser, M. 1993. Lipid domains in biological membranes. *Curr. Opin. Struct. Biol.* **3:** 475–481.
51. Yeagle, P. L. 1990. Role of cholesterol in cellular functions. *In* Advances in Cholesterol Research. M. Esfahani and J. B. Swaney, editors. The Telford Press Inc., Caldwell, NJ. 89–110.